Food Chemistry Advances 2 (2023) 100250

Contents lists available at ScienceDirect

Food Chemistry Advances

journal homepage: www.elsevier.com/locate/focha

Multilayer antimicrobial films based on starch and PLA with superficially incorporated ferulic or cinnamic acids for active food packaging purposes

Ramón Ordoñez*, Lorena Atarés, Amparo Chiralt

Instituto Universitario de Ingeniería de Alimentos para el Desarrollo, Universitat Politècnica de València, Camino de Vera, s/n, Valencia 46022, Spain

A B S T R A C T

Active packaging based on biodegradable polymers with naturally occurring active compounds, such as ferulic (F) and cinnamic (C) acids, have been studied to reduce the environmental impact of food packaging while prolonging food shelf-life. Three-layered films PLA/starch/PLA (PSP) were designed based on the complementary barrier properties of the polymers, and film systems with improved barrier properties were obtained. To promote the compound release, superficial incorporation of F or C through two coating methods was tested: film spraying with 5% ethanolic solutions of F or C and electrospinning of solutions containing PLA and active compound. Electrospinning was effective at producing fibre mats encapsulating the acids while the film spraying produced firmly attached crystalline formations of active compounds on the surface. Films coated by both electrospinning and pulverisation showed effective growth inhibition of *E. coli* and L. *innocua. Listeria* was more sensitive to both active compounds while C showed greater antibacterial activity. Electrospun films were more effective than pulverised, suggesting a greater ability to release the active compounds. Therefore, PSP laminates with surface-loaded ferulic or cinnamic acid are good materials for active food packaging, contributing to extending the food shelf life.

1. Introduction

Although a great effort to regulate the use of single-use petrochemical plastics has been made, the food packaging industry still relies on these materials given their great functional properties and low cost (Porta et al., 2020). To solve this crisis, biodegradable and renewably-sourced polymers, such as cassava starch or polylactic acid (PLA), have been exhaustively studied as economically viable alternatives to conventional plastics (Elvers et al., 2016; Mangaraj et al., 2018). Likewise, there is greater and greater consumer demand for a reduction in the synthetic additives in food products (Carocho et al., 2014), while food safety needs to be ensured. Active packaging is an innovative approach to extending food shelf-life by deliberately incorporating active components into the packaging material that would interact with the food product (Yildirim et al., 2018). Incorporating naturally-occurring antimicrobial or antioxidant agents into biodegradable polymers could bring renewable food packaging materials, meeting consumer demand and ensuring food safety (Mangaraj et al., 2018; Yildirim et al., 2018).

Thermoplastic starch films exhibit extensible and plastic behaviour and good oxygen barrier capacity, but poor water vapour barrier capacity and a high degree of water sensitivity and solubility, all of which represents a drawback to the wrapping of high-moisture foods (La Fuente Arias et al., 2021; Ordoñez et al., 2021; Zhong et al., 2020). In contrast, PLA is a hydrophobic renewable polyester, with relatively poor oxygen barrier capacity but high barrier capacity for water vapour and mechanical strength (Jamshidian et al., 2010). The properties of PLA films make them suitable for food packaging applications, and their production is becoming more economically viable (Elvers et al., 2016; Muller et al., 2017). Starch and PLA present complementary barrier properties, so multilayer assemblies of these two materials can offer great barrier properties both to water vapour and oxygen (Muller et al., 2017). Moreover, PLA external layers could potentially protect the inner layer of starch from moisture intake from the environment or the packaged food products.

Phenolic acids and their precursors are naturally-sourced antimicrobial and antioxidant agents that can be found in a wide range of plant species (Rashmi & Negi, 2020). Contrary to essential oil compounds, phenolic acids are not volatile and have a lower organoleptic impact on food matrices (Choi et al., 2018; W. Liu et al., 2021). Cinnamic and ferulic acids have been previously incorporated into starch matrices, exhibiting great antimicrobial activity against Gram + and Gram – bacteria (Ordoñez et al., 2021). However, given the limited applicability of hydrophilic starch films on high-moisture food products (Muller et al., 2017a), the incorporation of these active compounds into more hydrophobic matrices, such as PLA, could potentially result in highly applicable active food packaging materials. Nevertheless, previous studies (Ordoñez et al., 2022a, 2022b) using thermoprocessed or casting methods PLA films found no significant release of ferulic and cinnamic acids from the films into aqueous media, such as sensitive foods to microbial spoilage, which greatly limited their antimicrobial action. In contrast, subsequent studies (Ordoñez et al., 2022c) incorporating ferulic acid onto the PLA film surface or into fibre-structured electrospun mats demonstrated how effective this was at controlling the growth of *Escherichia coli* and *Listeria innocua*. The distribution of active compound

* Corresponding author.
E-mail addresses: raorla@doctor.upv.es (R. Ordoñez), loathue@tal.upv.es (L. Atarés), dchiralt@tal.upv.es (A. Chiralt).

https://doi.org/10.1016/j.focha.2023.100250
Received 28 October 2022; Received in revised form 21 February 2023; Accepted 21 March 2023

near the film surface was effective at promoting its antimicrobial action, thus avoiding the diffusion limitations of the compound through the PLA matrix, where the mass transfer process was greatly hindered due to the glassy state of the polymer and the lack of matrix relaxation when in contact with aqueous systems.

Electrospinning is a novel approach to obtaining nanofibres of polymeric materials with a high specific surface area that facilitates active compound release (Huang & Thomas, 2018). Electrospinning polymeric solutions with biodegradable polymers and naturally-occurring active compounds have been used as an efficient strategy to obtain fast active release rates (Quiles-Carrillo et al., 2019; Tampau et al., 2018; Yilmaz et al. 2022). Quiles-Carrillo et al. (2019) obtained PLA nanofibres encapsulating gallic which exhibited adequate compound release rates in saline media. Tampau et al. (2020) also produced PLA fibres encapsulating carvacrol, using food contact solvents, such as ethyl acetate and DMSO. In a previous study, the effectiveness of electrospun PLA materials with ferulic acid against *Listeria innocua* was found, hence revealing the release of the active compound from the fibrous mat (Ordoñez et al., 2022c).

The surface application of cinnamic and ferulic acids onto packaging films employing solution spraying also represents an easy method to prepare active packaging materials. These compounds exhibit high solubility in ethanol (Noubigh & Akremi, 2019; Shakeel et al., 2017) which is a cheap, safe and volatile solvent. Hence, the pulverisation of ethanolic solutions with F or C could lead to a quick surface oversaturation during solvent evaporation, triggering the surface crystallisation of the compounds (Batista et al., 2019; Chen et al., 2020). These crystalline structures could be initially attached to a PLA surface thanks to the tendency of PLA towards electric polarization and static electricity (Urbaniak-Domagala, 2013): once a small crystal is attached, it could grow if continuously exposed through the oversaturated stream. A previous study (Ordoñez et al., 2022c) revealed the effective release of crystallized ferulic acid from the PLA film surface when applied by pulverization of the compound ethanolic solution, which allowed for the antibacterial action of the compound against *Listeria innocua.*

This study aimed to develop biodegradable, active materials for food packaging purposes, with adequate barrier capacity to oxygen and water vapour, useful to extend the food shelf life. To this end, PLA and starch were laminated as three-layer assemblies, with two PLA outer layers to protect the internal starch layer from moisture. The functional and structural properties of the mono and three-layer were characterised. To provide the three-layer with active properties, ferulic and cinnamic acids were incorporated onto the food contact PLA surface of the tri-layer by using two different methods: electrospinning of PLA-active solutions and pulverisation of ethanolic solutions of the active compounds. The antibacterial properties of these materials were evaluated to validate these three-layer active properties.

2. Materials and methods

2.1. Materials

Amorphous PLA 4060D (106 kDa MW, Nature Works, MN, USA), cassava starch (Asia Co., LDT, Kalasin, Thailand) and glycerol (Panreac Química, Barcelona, Spain) were used to formulate film monolayers. Magnesium nitrate and phosphorus pentoxide supplied from Panreac Química were used to control relative humidity (RH) for film conditioning purposes. Cinnamic (C) and ferulic (F) acids were used as active components and were purchased from Sigma-Aldrich (Saint Louis, USA). Ethyl acetate, from Indukern (Barcelona, Spain), and dimethyl sulfoxide (DMSO), from Panreac Química, were used as solvents in the electrospinning solutions. Ethanol (96%), from Panreac Química, was used as the solvent for pulverisation solutions. Tryptone soy broth, bacteriological agar, and peptone water obtained from Scharlab (Barcelona, Spain) were used for antibacterial tests. Bacterial strains, *Listeria innocua* (CECT 910) and *E. coli* (CECT 101) were supplied by the Spanish Type Collection (CECT, University of Valencia, Spain). Selective media: violet-red bile agar (VRBA) for *E. coli* and palcam agar base (PAB) enriched with palcam selective supplement for *Listeria* were obtained from Scharlab.

2.2. Film preparation

Starch and PLA monolayers were obtained separately and assembled in three-layer systems with two outer PLA layers enclosing an inner starch sheet; ferulic or cinnamic acid was incorporated by electrospinning or the surface pulverization of one of the PLA sheets.

2.2.1. Starch and PLA monolayers

The starch monolayers were prepared according to previous studies (Ordoñez et al., 2021). Cassava starch was melt-blended with glycerol at 0.3 g/ g starch ratio in an internal mixer (Haake PolyLab QC, Thermo Fisher Scientific, Germany) at 130 °C and 50 rpm for 10 min. The obtained melts were ground with an M20 IKA mill (Staufen, Germany) and conditioned for 1 week inside a desiccator at 53% RH, using $MgNO_3$ oversaturated solution, at 25 °C. The samples (4 g) were placed onto 20 cm diameter Teflon moulds to obtain films of the same diameter by compression-moulding, using a hot-plate hydraulic press (LP20, Labtech engineering, Thailand). The samples were preheated at 160 °C for 1 min and subsequently compressed at 5 MPa for 2 min, followed by a second compression at 10 MPa. Finally, a cooling step to 70 °C in 3 min was applied. The films were stored at 53% RH and 25 °C until their use.

The PLA monolayers were obtained using the previously described conditions (Muller et al., 2017). PLA pellets were cold ground and 2 g samples were placed onto 20 cm diameter Teflon moulds to be compression moulded. An initial preheating step took place at 200 °C for 4 min before a 10 MPa compression at the same temperature for another 4 min, ending with a cooling step to 70 °C for 3 min.

2.2.2. Multilayer assembly

The multilayer films were obtained by the thermo-compression of two external PLA layers and one inner starch layer (PSP). All three monolayers, in the abovementioned arrangement inside the heating hydraulic press, were preheated for 2 min at 110 °C and then compressed at 2.5 MPa and 110 °C for 1 min before being cooled to 70 °C for 3 min. No irregularities and good layer adhesion were observed in these conditions.

Both monolayers and PSP assemblies were characterised by their functional properties. Likewise, PSP films were surface coated with ferulic or cinnamic acid by spraying or electrospinning, as described below, and tested as to their antimicrobial activity.

2.3. Characterisation of the film properties

2.3.1. Tensile properties

A TA-XT plus (Stable Micro Systems, Haslemere, England) texture analyser was used to measure the tensile properties of each film formulation, following the ASTM D882 method (American Society for Testing Materials, 2002). Film samples of 25 mm x 100 mm were cut (eight replicates per formulation) and their thickness was determined at six random points using an electronic digital micrometre (Comecta S.A., Barcelona, Spain). The samples were mounted on tensile grips (50 mm separation) and stretched at 50 mm/min. Tensile strength at break (TS), elastic modulus (EM) and elongation at break (%E) were calculated from the stress-Henky strain curves.

2.3.2. Thermal properties

The thermal properties of the PSP assemblies and the monolayers were studied using a differential scanning calorimeter (DSC, 1 StareSystem, Mettler-Toledo, Switzerland) and a thermogravimetric analyser (TGA/SDTA 851e, Mettler-Toledo, Switzerland). The samples were conditioned at 0% RH in desiccators with P_2O_5 before the tests. The DSC

analysis consisted of the following steps: cooling from room temperature to −10 °C at 10 K/min, heating to 160 °C at the same heating rate, maintaining 160 °C for 5 min, cooling at 50 K/min to −10 °C, maintaining −10 °C for 5 min, and heating back to 160 °C at 10 K/min. An empty aluminium pan was used as a reference. For TGA analyses, 10 mg samples in alumina crucibles were heated from 25 to 600 °C at 10 K/min, under a nitrogen flow (50 mL/min). Both tests were performed twice per formulation.

2.3.3. Barrier properties

The water vapour permeability (WVP) was determined following the ASTM E96–95 method (American Society for Testing Materials, 1995). Payne permeability cups (3.5 cm diameter, Elcometer SPRL, Hermelle/s Argenteau, Belgium) were filled with 5 ml of distilled water and covered with circular film samples whose thickness had been previously measured at six random points. The cups were placed into desiccators containing $MgNO_3$ oversaturated solution inside a temperature-controlled chamber at 25 °C. Cups were weighed periodically at one-hour intervals, starting after 16 h in the chamber, using an analytical balance (±0.00001 g). The weight loss rate *vs.* time data, in the stationary state, were used to calculate WVP, following the E96–95 method, as described by Andrade et al. (2020). Three replicates were obtained per formulation.

Oxygen permeability (OP) was measured following the ASTM D3985–05 method (American Society for Testing Materials, 2010) employing an Ox-Tran 1/50 equipment (Mocon, Minneapolis, USA). The film test area was 50 cm^2 and measurements were taken at 25 °C and 53% RH. The OP was calculated by dividing the oxygen transmission rate by the oxygen partial pressure gradient on both sides of the film and multiplying by the average film thickness, which was previously measured at six different positions of the film sample. Two replicates per formulation were obtained.

2.3.4. Optical properties

The optical properties of the films were analysed with a CM-5 spectrocolorimeter (Konica Minolta, Inc., Japan). The reflection spectra (400–700 nm) were obtained for three film replicates and at three points per replicate, backed on both black and white plates. The internal transmittance (T_i) was calculated by applying the Kubelka-Munk theory of multiple dispersion (Hutchings, 1999). The CIEL*a*b* colour coordinates were obtained from the determined reflectance of an infinitely thick layer of material, considering the D65 illuminant and 10° observer (Cano et al., 2014). Finally, the lightness (L*), chroma (C_{ab}*) and hue (h_{ab}*) psychometric coordinates were calculated (Mahy et al., 1994).

2.4. Coating of three-layered PSP with active compounds

To obtain active PSP laminates, the trilayers were coated on one of the PLA external layers with ferulic or cinnamic acid using two alternative procedures: the electrospinning of PLA-active solutions or by the direct spraying of ethanolic solutions of the actives.

2.4.1. Electrospinning of active PLA solutions

Based on previous studies (Ordoñez et al., 2022c; Tampau et al., 2020), polymeric solutions for the electrospinning process were formulated using an ethyl acetate-DMSO blend (Ratio 6:4) as a food-grade solvent. The PLA concentration was 15 g/100 g solution and ferulic or cinnamic acid was added at 15 g/100 g solids. The solutions were electrospun in a Fluidnatek LE-10 (Bioinicia SA, Valencia, Spain) setup, with 5 mL syringes (BD Plastik) as solution container and a 0.6 mm stainless steel needle at the spinneret. The operation conditions were adjusted empirically based on the formation of a stable Taylor cone in the solution stream. The collector-syringe distance was fixed at 20 cm, the flow rate at 2500 μL/h and the voltage range from 12 to 14 KV. The PSP film samples were placed on the collector and a continuous stream was electrospun for 75 min in order to achieve a theoretical active concentration of 0.45 mg/cm^2 on the film surface. After the electrospinning process, annealing was subsequently applied to the coated films to promote the compaction of the fibre mats and to ensure good adhesion to the PSP films. To this end, the films were placed inside the hydraulic hot-plate press, between steel plates, and heated at 50 °C for 1 min, without additional pressure.

2.4.2. Superficial pulverisation of active solutions

Cinnamic or ferulic acid was pulverised on the surface of PSP films employing an airbrush (E4182, Elite pro) loaded with 5% w/v active solutions in 96% ethanol. Circular film samples of 5.5 cm were placed at a vertical distance of 14.7 cm below the airbrush nozzle and were sprayed at 8 μL/s flow for 5 s. After pulverisation, the samples were vacuum dried at 60 °C and 0.1 atm overnight.

2.5. Active compound quantification

The ferulic and cinnamic acid contents of three-layered PSP were obtained by methanolic extraction and UV–visible spectrophotometry. The dry samples (100 mg) were immersed in 10 ml of methanol and kept under magnetic stirring at room temperature for 72 h. The absorbence measurements for F and C were taken at 320 nm and 270 nm, respectively, after filtration and proper dilution. A similarly extracted sample without actives was used as blank. A previously determined methanol calibration curve for each active compound was used to quantify the concentration of ferulic or cinnamic acid in the films. Results were expressed in mg of active per film unit area.

2.6. Microstructural analyses

A high-resolution field emission scanning electronic microscope (HR-FESEM) (GeminiSEM 500, Zeiss, Germany) was used to observe the superficial and cross-section microstructures of the obtained materials. The samples were cryofractured using liquid nitrogen (only for cross-section observations), mounted in supports with carbon tape and platinum-coated before observation. ImageJ software (v.153c, National Institute of Health, Bethesda, USA) was used for image analysis.

2.7. Antibacterial activity assessment

The antibacterial capacity of the active coated films was assessed through the growth inhibition of L. *innocua* and *E. coli,* according to previous studies (Ordoñez et al., 2021; Tampau et al., 2018). The sterilised media, materials and film samples were placed inside a laminar flow cabinet (Bio II advance, Telstar, Spain) and exposed to UV light for 15 min. The Petri dishes (55 mm diameter) were filled with 10 mL of TSA media and left to solidify before being inoculated with 100 μL of a bacterial suspension at 10^5 CFU/mL in order to obtain an initial concentration of 10^3 CFU/mL in the plate. The TSA was covered with the film's active surface, and the plates were sealed. All the films were tested in duplicate. After 6 days of incubation at 10 °C, the samples were homogenised in 100 mL of peptone water using a paddle masticator (IUL Instruments, Barcelona, Spain) and serial dilutions were plated (in duplicate) in selective growth media: Palcam agar base enriched with *Listeria* selector for L. *innocua,* and red vile agar for *E. coli*. After 48 h of incubation at 37 °C, the colonies were counted and compared with the uncoated growth control samples.

2.8. Statistical analysis

Data statistics were evaluated through a one-way analysis of variance (ANOVA) using Statgraphics Centurion XVIII software. Fisher's least significant difference was used at a 95% confidence level.

3. Results and discussion

3.1. Properties of the PSP laminates

3.1.1. Structural properties

Multilayer films were successfully assembled, exhibiting good adhesion between layers, without irregularities. These were characterised by their main functional properties as packaging material, in comparison with their constitutive monolayers, as shown in Table 1. The three-layered PSP was not as thick as the sum of the individual thicknesses of the monolayers (a reduction of approximately 25%), which indicates that additional radial flow occurred in the different sheets during the adhesive thermo-compression step, reducing the final thickness of the three-layered PSP. The individual reduction of each polymer sheet was estimated from the cross-sectional observations by FESEM (Fig. 1). Comparing the initial monolayer thickness with that measured in the three-layered assemblies (about 90 and 170 μm for PLA and starch layers, respectively), a greater thickness reduction was observed for PLA than for starch monolayers, coherently with the higher degree of flowability of PLA. Similar results were observed by other authors for starch-polyester bilayers during the thermo-compression step (Hernández-García et al., 2021).

Table 1
Properties of PLA and starch monolayers, and PSP multilayer assemblies. Film thickness (t), tensile strength (TS) and elongation at break (E%), elastic modulus (EM); glass transition temperature (Tg) from the second heating scan, thermal degradation temperature (onset (T_{onset}) and peak (T_{peak})), water vapour transmission rate (WVTR), oxygen transmission rate (OTR), colour parameters (lightness (L^*), hue (hab^*), chroma (Cab^*)) and internal transmittance (Ti) at 400 and 700 nm.

	PLA	Starch	PSP
t (μm)	129±6^a	211±8^b	352±20^c
TS (MPa)	29.2 ± 0.8^b	2.8 ± 0.4^a	29.0 ± 2.0^b
EM (MPa)	1510±40^c	40±8^a	1030±70^b
E (%)	2.9 ± 0.4^a	19.2 ± 0.2^c	8.0 ± 2.0^b
Tg_{PLA} (°C)	54±2^a	–	50±3 ^{a}
Tg_{Starch} (°C)	–	100±9^a	100±5^a
T_{onset} (°C)	265±3^b	246±2^b	247±2^b
T_{peak} (°C)	309±2^b	280±2^a	308±2^b
WVTR (g/kPa·h·m^2)	1.28±0.05^b	59±6^c	0.12±0.01^a
OTR x 10^{-18} (cm^3/m^2·s·Pa)	96.9 ± 1.1^c	3.1 ± 0.2^a	7.12±0.12^b
L^*	82.4 ± 0.7^c	61.5 ± 3.1^b	59.2 ± 1.1^a
$h_{ab}{}^*$	99.0 ± 3.0^c	74.0 ± 0.1^a	76.7 ± 0.5^b
$C_{ab}{}^*$	7.4 ± 1.1^a	11.4 ± 0.6^b	13.9 ± 0.3^c
Ti (400 nm)	0.89±0.02^b	0.78±0.02^a	0.80±0.01^a
Ti (700 nm)	0.92±0.02^a	0.88±0.01^a	0.90±0.01^a

Different superscript letters indicate significant differences between film formulations ($p < 0.05$).

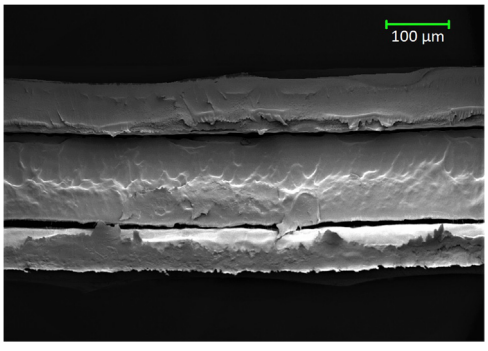

Fig. 1. Cross-sectional HR-FESEM observation of PSP trilayer assemblies. (1.00 kV; magnification: X150).

3.1.2. Tensile properties

The tensile behaviour of three-layered films, compared with the monolayers, is shown in Fig. 2**a**. The lower strength and more plastic behaviour of the starch layer can be observed, as compared with the stiffer and more brittle PLA films, as previously reported (Collazo-Bigliardi et al., 2019; Muller et al., 2017). As expected, three-layered assemblies exhibited similar strength to PLA monolayers, but with enhanced plastic deformation. In general, the rupture of the PSP films during stretching occurs when the PLA layers break while the internal starch sheet is still becoming longer, as can be observed in Fig. 2**a**. The tensile parameters, elastic modulus, tensile strength and deformation at break are shown in Table 1 for PSP assemblies and monolayers, in which it can be observed that PSP presented the same resistance to break (TS) as the PLA monolayers. The PLA layers offered the three-layered structure great resistance and stiffness, whereas the stretchability was better in the three-layered structure than in the PLA films. This effect suggests that the PLA in contact with starch could be partially hydrolysed, gaining plasticity and slightly reducing its stiffness. Therefore, combining PLA and starch layers in multilayer assemblies implied a significant improvement in the mechanical performance of the material, better meeting the food packaging requirements than the individual films. The partial migration of glycerol and water molecules from the starch layer to the PLA matrix could modify the PLA's tensile behaviour in the multilayer. The high degree of sensitivity of PLA to hydrolysis in the presence of the migrated water (Rocca-Smith et al., 2017) would largely explain the observed behaviour. The hydrolysed oligomers could plasticise the PLA sheets making them more stretchable.

3.1.3. Thermal behaviour

The DSC analyses of monolayers in the second heating scan (Fig. 3**a**) showed the typical glass transition of amorphous PLA and thermoplastic cassava starch, with midpoint Tg values at 54 °C and 100 °C, respectively, which agrees with that previously reported for these polymers (Collazo-Bigliardi et al., 2019; Muller et al., 2017). For the three-layered assembly, thermograms also exhibited both glass transitions, with no significant changes in the Tg values. For the PLA, a decreasing trend in the Tg value was observed in the three-layered structure which could be explained by the partial migration of the plasticiser or the water hydrolysis effect, as previously commented on. Likewise, the thermodegradation pattern of the three-layered structure was similar to the monolayers (Fig. 3**b**), exhibiting overlapped thermal degradation of both polymers due to the similar temperature at which this occurs in both cases. PLA is slightly more thermostable than starch and the obtained degradation temperature values were in the range of those previously reported by other authors for these polymers (Collazo-Bigliardi et al., 2019; Muller et al., 2017). The degradation temperatures of both materials overlapped in a single degradation curve starting at the starch onset temperature and exhibiting the peak degradation near the sole PLA peak temperature, as observed by other authors (Collazo-Bigliardi et al., 2019; Gómez-Contreras et al., 2021) for PLA/Starch blends.

3.1.4. Barrier properties

As concerns the barrier properties, the water vapour transmission rate (WVTR) and oxygen transmission rate (OTR) are shown in Table 1. The starch and PLA monolayers exhibited similar values to those previously reported for PLA and starch films (Collazo-Bigliardi et al., 2019; Ordoñez et al., 2021); the starch layer exhibited a good oxygen barrier capacity whereas PLA exhibited good barrier capacity to water vapour. The PSP assemblies exhibited a highly reduced water vapour transmission rate with respect to the starch films, as well as a reduced oxygen transmission rate with respect to the PLA films. Thus, this material presented an improved overall barrier capacity for water vapour and oxygen. This is coherent with the additive effect of the assembled parallel resistances to mass transfer offered by the layer combination. Applying the mass transfer model for successive resistances assembled perpendicularly to the mass flow (eq. (1)), and considering the thickness

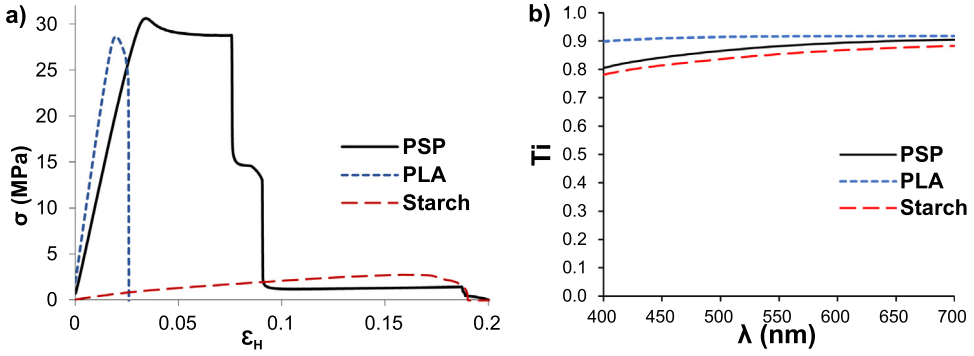

Fig. 2. a) Strain-stress curves and **b)** Internal transmittance (Ti) spectra of PLA and starch monolayers and PSP multilayer assemblies.

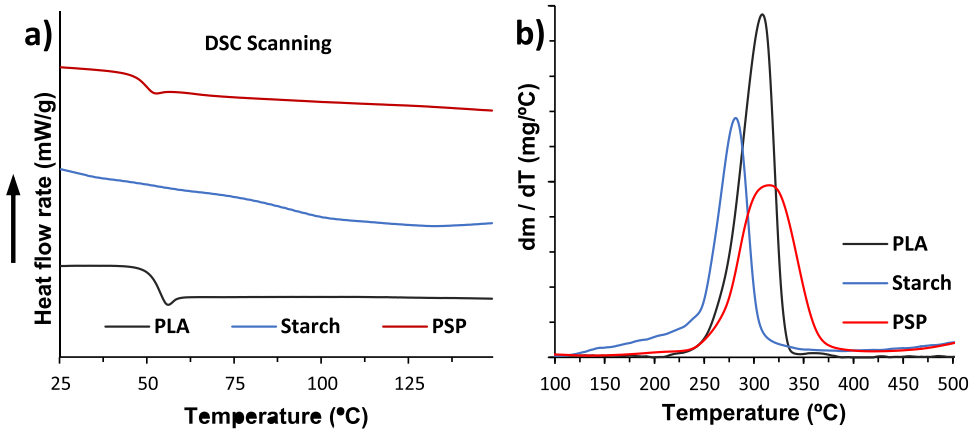

Fig. 3. Thermal properties of PLA and starch monolayers and PSP multilayer films: **a)** DSC heating thermograms and **b)** Derivative TGA curves.

of the different layers in the three-layered assembly, the values of the WVTR and the OTR were 2.5 g/kPa.h.m^2 and 6.2 × 10^{18} cm^3/Pa.s.m^2, respectively, which indicates that the experimental OTR values practically meet the model predictions, whereas the experimental WVTR was 20 times lower than the predicted value. This additional improvement in the water vapour barrier capacity of PSP films could be attributed to the interfacial interactions of the PLA-S layers that could confer more barrier capacity onto the multilayer assembly. Likewise, the gradient of water vapour established in the monolayer starch films during the WVTR measurements may be different than that established in the internal starch layer when the measurement was taken in the PSP films, thus affecting the obtained value. This also demonstrates the protective effect of the PLA sheet against the moisturising of the internal starch. In contrast, with PLA being more permeable to oxygen than starch, the external PLA layer did not significantly limit the oxygen flow or the establishment of the corresponding oxygen gradient in the starch sheet.

$$\frac{t_{ML}}{TR_{ML}} = \sum_i \frac{t_i}{TR_i} \quad (1)$$

Where t is the thickness of the multilayer (ML) or each layer (i) and TR is the transmission rate of the multilayer (ML) or each layer (i).

3.1.5. Optical properties

The colour coordinate values for the PSP assemblies and monolayers are shown in Table 1. The monolayers exhibited similar colour parameter values to those previously reported for starch or PLA films (Ordoñez et al., 2021, 2022a, 2022b), the starch layer being slightly darker and redder. The multilayer assembly, however, presented similar colour parameter values to the starch films, as expected from the parallel arrangement of the layers. This behaviour was corroborated by the internal transmittance spectra (Fig. 2**b**), where the PSP assembly exhibited very similar internal transmittance spectra to the starch films but with slightly higher values due to the reduction in the thickness of the starch sheet during the adhesive thermo-compression process, as observed by Muller et al. (2017). Therefore, the three-layered assembly exhibited slightly greater transparency than starch monolayers with colour parameters similar to those of the starch monolayers.

3.2. Superficial incorporation of ferulic and cinnamic acids on PSP laminates

The active compounds were successfully incorporated onto the surface of the PSP assembly by electrospinning or solution pulverisation. The microstructure of the electrospun mats over the films was observed by HR-FESEM, and the images are shown in Fig. 4**a**. In both cases, fibre mats were obtained, as observed in a previous study (Ordoñez et al., 2022c) for ferulic acid-PLA solutions using DMSO:EtAc (6:4) solvent. Electrospun mats with ferulic acid were highly fluffy and were submitted to the annealing process to favour their compaction and good adhesion to the PLA surface, as described in the methods section. This was not required in PLA-cinnamic acid mats, which exhibited a denser structure well adhered to the PLA film surface. In Fig. 4**a**, the final structure of the electrospun mats encapsulating ferulic and cinnamic acids can be observed, where the more open nanofibre structure can be seen for samples with ferulic acid, despite the annealing treatment. This structural difference could be due either to the effect of cinnamic acid on PLA fibres, inhibiting their repulsive interactions, or to the higher degree of solvent retention, leading to the depositing of not completely dry PLA fibres on the mat, as observed by other authors for PLA-carvacrol electrospun materials from DMSO solutions (Tampau et al., 2020). Solvent retention in the electrospun material could favour both fibre adhesion and flattening when deposited on the collector. In both cases, the high specific surface area of the fibre structure could enhance the release rate of the active compounds (Huang & Thomas, 2018). The image analysis in the micrographs revealed a similar fibre diameter for both ferulic and cinnamic acids, encapsulating fibres with 1.5 ± 0.1 μm and 1.5 ± 0.3 μm, respectively. The cross-sectional HR-FESEM observations of the PSP

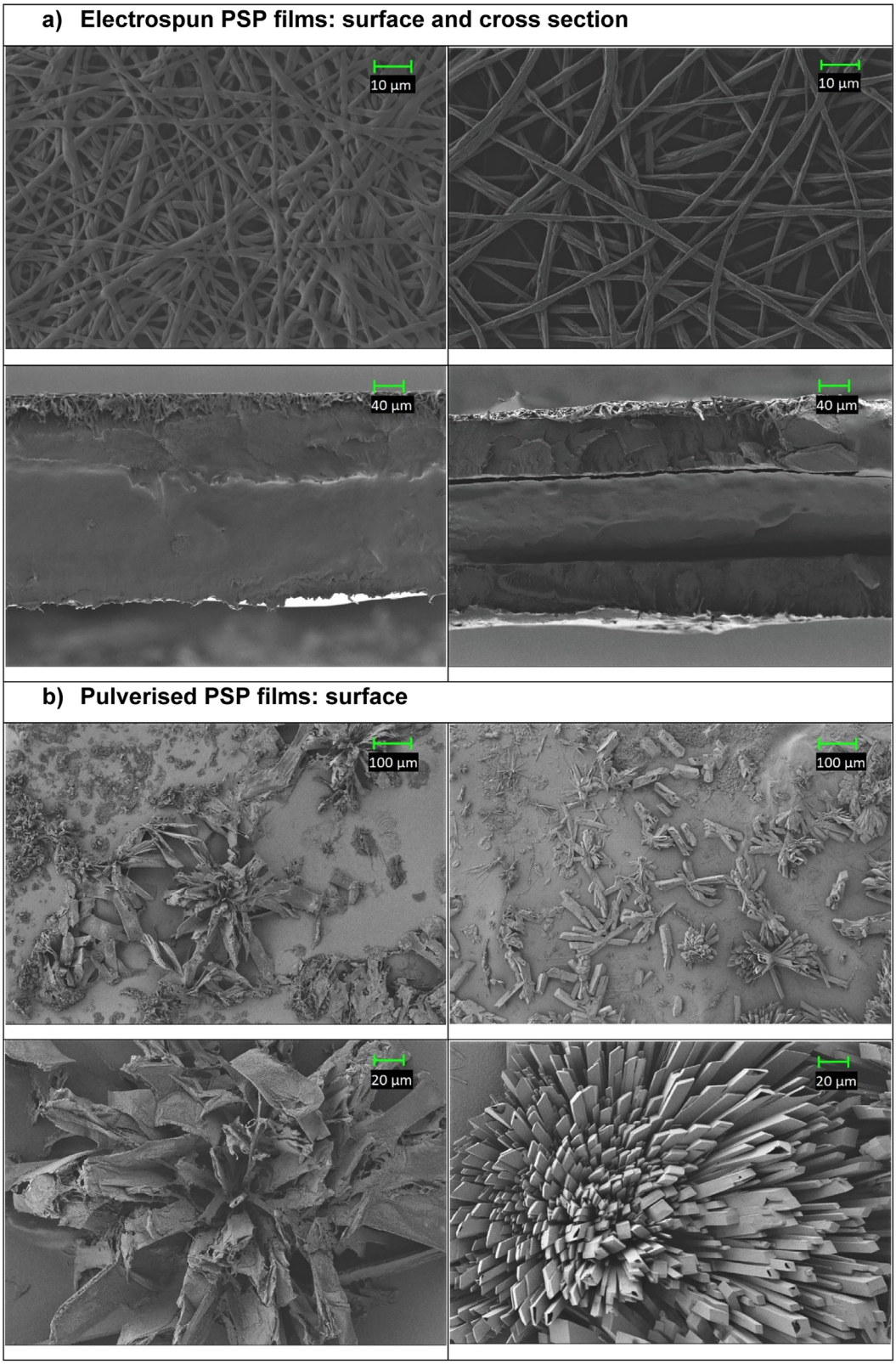

Fig. 4. HR-FESEM images (1.00 kV) of PSP films containing cinnamic acid (left) or ferulic acid (right) **a)** electrospun PLA fibres with ferulic or cinnamic acid on the surface of the PSP multilayer (x1000) and cross-sections of the coated PSP films (x200) and **b)** Crystalline structures of cinnamic or ferulic acid on the surface of superficially pulverised PSP multilayer films.

Table 2
Superficial concentration of ferulic (F) and cinnamic (C) acids in the electrospun (ES) and pulverized (P) PSP films, theoretical concentration in the culture plate (TCCP), assuming a complete release from the different films, and growth inhibition of *E. coli* and L. *innocua* with respect to the uncovered control samples, obtained in the *in vitro* tests with the different PSP materials.

Formulation	Surface concentration (mg/cm^2)	TCCP (mg/mL)	*E. coli* growth inhibition (Log (CFU/mL))	L. *innocua* growth inhibition (Log (CFU/mL))
ES-C	0.44±0.02	1.04	2.6 ± 0.2^b	7.3 ± 0.8^c
ES-F	0.40±0.03	0.95	1.4 ± 0.3^a	6.1 ± 0.4^c
P-C	0.52±0.06	1.23	2.3 ± 0.2^b	4.3 ± 0.2^b
P-F	0.48±0.08	1.14	1.3 ± 0.1^a	2.5 ± 0.4^a

Different superscript letters indicate significant differences between film formulations ($p < 0.05$).

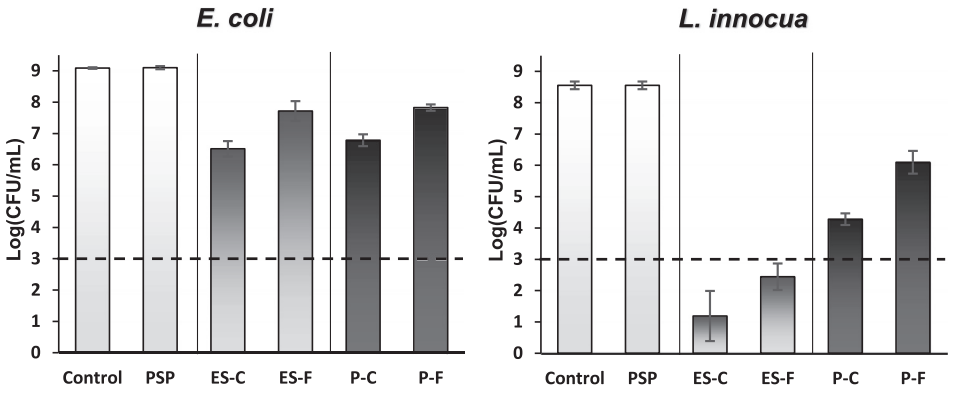

Fig. 5. Bacterial growth obtained from *in vitro* tests after 6 days of incubation at 10 °C for plates coated with PSP multilayers with and without cinnamic (C) or ferulic (F) acid superficially incorporated by electrospinning (ES) or pulverisation (P). The control bar shows the mean growth for uncoated plates and the dotted line represents initial inoculation.

films coated with the acid-loaded fibres are shown in Fig. 4**a**, where the good adhesion of the electrospun mats to the film surface can be observed.

Pulverised solutions of ferulic or cinnamic acid on the PSP surface gave rise to the formation of crystalline structures of the respective acid, which were well attached to the PLA surface after the solvent evaporation, as can be observed in the HR-FESEM micrographs of the film surface (Fig. 4**b**). Ferulic acid crystalline agglomeration structures were similar to those observed by Chen et al. (2020). These authors reported that ferulic acid tends to agglomerate in needle-like structures when precipitated in oversaturated solutions. Thus, the fast solvent evaporation in pulverised films promoted the crystallisation of ferulic acid on the film surface, forming well-adhered crystalline structures. Batista et al. (2019) also studied the crystallisation of cinnamic acid, observing similar crystalline structures but smaller in size. Due to the crystallisation, no homogeneous distribution of cinnamic acid could be observed on the film surface, but agglomerations of crystalline forms of differing sizes in highly intricate structures that could affect the release rate of active compounds when the coated film is put into contact with an aqueous medium, such as an inoculated culture or real food matrices. In fact, the solubilisation rate of the active compound in the aqueous media may be affected by the crystalline structure and crystal sizes (Batista et al., 2019). Even distribution and a smaller, homogeneous size of crystals could be achieved by changing the solvent or spraying conditions, such as nozzle type or flow.

The contents of active compounds incorporated onto the PSP films, determined by methanolic extraction and spectrophotometric quantification, are shown in Table 2 for both electrospun (ES) and pulverized (P) PSP films. Although the surface concentration (mg/cm^2) reached similar values for both treatments, it was slightly higher for the pulverised samples. By taking these contents, the film area and volume of the culture medium in the plates into consideration, the theoretical concentration of both active compounds in the culture medium was estimated, assuming their complete release. These values were very close to 1 mg/mL, according to the target concentration established as necessary to reach the minimal inhibitory concentration (MIC) of the bacteria in the antimicrobial test. According to a previous study (Ordoñez et al. 2021), the MIC values of L. *innocua* were 0.70 and 0.65 mg/mL for ferulic and cinnamic acids respectively, while for *E. coli* these were 0.80 and 0.70 mg/mL, for FA and CA respectively. Therefore, the MIC of both active compounds for the bacteria would be exceeded in all cases if their complete release is achieved in the culture medium.

3.3. Antibacterial activity of PSP films surface loaded with ferulic or cinnamic acid

Fig. 5 shows the bacterial counts for *E. coli* and L. *innocua* after 6 days of incubation at 10 °C for the different active PSP materials coating the culture plates, and compared with the control uncoated plates and those coated with PSP films without active compounds. In Table 2, the growth inhibition values concerning the control samples are shown. All the films coated with active compounds, by spraying or electrospinning, inhibited the growth of both *E. coli* and L. *innocua* to a different extent, depending on the active compound, the bacterial strain and the active incorporation method. This revealed that the extent of the effective release of the incorporated compounds into the culture medium was enough to reach the corresponding MIC values. Both F and C were more effective at controlling the growth of L. *innocua* than *E. coli*, coherently with the lower MIC values of L. *innocua* with both compounds (Ordoñez et al., 2021), Gram-negative such as *E. coli* are expected to be more resistant to antimicrobials, as their outer membrane is very challenging for small molecules to cross (Liu et al., 2020). In the same way, cinnamic acid was more effective than ferulic acid, also coherently with the lower MIC values of this compound for both strains the lower antibacterial activity of F could be attributed to its -OH in the aromatic ring, which reduces its lipophilic character and, thus, its ability to interact with bacterial membranes (Campos et al., 2009; Miyague et al., 2015). These results agree with those obtained in a previous study (Ordoñez et al. 2021) where both compounds were incorporated into thermoprocessed starch films and tested as to their antibacterial capacity with the same strains. As concerns the incorporation method, different behaviour was observed for *E. coli* and L. *innocua*. No significant differences in the inhibition capacity of pulverised or electrospun films were observed for *E. coli*, whereas electrospun films were more effective than pulverised at inhibiting the growth of L. *innocua*, even though they contained a slightly lower concentration of active compounds. This indicates that releasing

the incorporated compounds from the electrospun mats coating the PSP films was more effective than doing so from the crystalline coating obtained by pulverisation. The different release rates had a significant effect on the more sensitive bacteria (L. *innocua*) but did not notably affect the growth inhibition of the less sensitive bacteria (*E. coli*). Electrospun PSP films containing cinnamic acid exhibited a bactericidal effect on L. *innocua*, reducing the initial inoculum after 6 incubation days, while films with electrospun ferulic acid exhibited a bacteriostatic effect due to it being less active against this bacteria. Quiles-Carrillo et al. (2019) also observed an adequate release of gallic acid from PLA electrospun fibres, reporting the main role of the active accumulated on the fibre surface that is easily releasable in contact with aqueous systems.

Therefore, electrospun PLA fibres loaded with active compounds, such as ferulic or cinnamic acid, were very effective at promoting the release of actives from their high specific surface area, providing the food packaging with active properties to extend the food shelf life. The pulverisation of concentrated solutions of these active compounds on the packaging material is a method that is both more easily available and cheap. However, the surface crystallisation of the compounds could limit their solubility in the microbially sensitive aqueous systems, making them less effective in terms of their antimicrobial action. Nevertheless, other solvents and pulverisation conditions should be studied to optimise the release of actives in order to favour antibacterial activity.

4. Conclusions

Three-layered PSP assemblies exhibited an improved mechanical and barrier capacity compared to the PLA and starch monolayer films with adequate functional properties to meet food packaging requirements. PLA provides the laminates with mechanical resistance and water vapour barrier capacity while the internal starch layer was protected from moisture sensitivity by the external PLA sheets, providing the laminates with oxygen barrier capacity. The incorporation of ferulic and cinnamic acids onto the PSP surface by electrospinning produced high specific surface fibre mats with release capacity of the active compounds as well as the crystalline structures of ferulic or cinnamic acid, resulting from the film spraying. The surface-loaded PSP laminates with F or C exhibited effective growth inhibition of *E. coli* and L. *innocua*, the latter being more sensitive to both active compounds and cinnamic acid showing greater antibacterial activity. For the more sensitive bacteria (L. *innocua*), the electrospun films were more effective than the pulverised, thus indicating their greater ability to release the active compounds into the culture medium. Therefore, laminates of PLA/starch/PLA surface loaded with ferulic or cinnamic acid are suitable materials for active packaging to extend food shelf life. Nonetheless, further studies into their stability and specific applications in real foods are necessary in order to determine their industrial feasibility.

Declaration of Competing Interest

The authors declare that they have no known competing financial interests or personal relationships that could have appeared to influence the work reported in this paper.

CRediT authorship contribution statement

Ramón Ordoñez: Investigation, Conceptualization, Methodology, Formal analysis, Writing – original draft, Writing – review & editing. **Lorena Atarés:** Conceptualization, Methodology, Data curation, Writing – original draft, Writing – review & editing, Supervision. **Amparo Chiralt:** Conceptualization, Methodology, Data curation, Writing – review & editing, Supervision, Project administration.

Data availability

Data will be made available on request.

Acknowledgments

The authors thank the Agencia Estatal de Investigación (Ministerio de Ciencia e Innovación, Spain) for the financial support through project PID2019-105207RB-I00.

References

American Society for Testing Materials. (1995). Standard test methods for water vapor transmission of materials. *Annual Book of ASTM Standards, 15*(C), 745–754. 10.1520/E0096.

American Society for Testing Materials. (2002). D 882: Standard test method for tensile properties of thin plastic sheeting. *Annual Book of ASTM Standards, 14*, 1–10.

American Society for Testing Materials. (2010). D3985-05 oxygen gas transmission rate through plastic film and sheeting using a coulometric sensor. *Annual Book of ASTM Standards, C*, 1–7. 10.1520/D3985-05.2.

Andrade, J., González-Martínez, C., & Chiralt, A. (2020). Effect of carvacrol in the properties of films based on poly (vinyl alcohol) with different molecular characteristics. *Polymer Degradation and Stability, 179*, Article 109282. 10.1016/j.polymdegradstab.2020.109282.

Batista, R. S., de, A., Melo, T. B. L., dos Santos, J. A. B., de Andrade, F. H. D., Macedo, R. O., et al., (2019). Evaluation of crystallization technique relating to the physicochemical properties of cinnamic acid. *Journal of Thermal Analysis and Calorimetry, 138*(5), 3727–3735. 10.1007/s10973-019-08455-7.

Campos, F. M., Couto, J. A., Figueiredo, A. R., Tóth, I. V., Rangel, A. O. S. S., & Hogg, T. A. (2009). Cell membrane damage induced by phenolic acids on wine lactic acid bacteria. *International Journal of Food Microbiology, 135*(2), 144–151. 10.1016/j.ijfoodmicro.2009.07.031.

Cano, A., Jiménez, A., Cháfer, M., Gónzalez, C., & Chiralt, A. (2014). Effect of amylose:Amylopectin ratio and rice bran addition on starch films properties. *Carbohydrate Polymers, 111*, 543–555. 10.1016/j.carbpol.2014.04.075.

Carocho, M., Barreiro, M. F., Morales, P., & Ferreira, I. C. F. R. (2014). Adding molecules to food, pros and cons: A review on synthetic and natural food additives. *Comprehensive Reviews in Food Science and Food Safety, 13*(4), 377–399. 10.1111/1541-4337.12065.

Chen, H., Wang, C., Kang, H., Zhi, B., Haynes, C. L., Aburub, A., et al., (2020). Microstructures and pharmaceutical properties of ferulic acid agglomerates prepared by different spherical crystallization methods. *International Journal of Pharmaceutics, 574*, Article 118914. 10.1016/J.IJPHARM.2019.118914.

Choi, I., Lee, S. E., Chang, Y., Lacroix, M., & Han, J. (2018). Effect of oxidized phenolic compounds on cross-linking and properties of biodegradable active packaging film composed of turmeric and gelatin. *Lwt, 93*(March), 427–433. 10.1016/j.lwt.2018.03.065.

Collazo-Bigliardi, S., Ortega-Toro, R., & Chiralt, A. (2019). Using grafted poly(ε-caprolactone) for the compatibilization of thermoplastic starch-polylactic acid blends. *Reactive and Functional Polymers, 142*(February), 25–35. 10.1016/j.reactfunctpolym.2019.05.013.

Elvers, D., Song, C. H., Steinbüchel, A., & Leker, J. (2016). Technology trends in biodegradable polymers: Evidence from patent analysis. *Polymer Reviews, 56*(4), 584–606. 10.1080/15583724.2015.1125918.

Gómez-Contreras, P., Contreras-Camacho, M., Avalos-Belmontes, F., Collazo-Bigliardi, S., & Ortega-Toro, R. (2021). Physicochemical properties of composite materials based on thermoplastic yam starch and polylactic acid improved with the addition of epoxidized sesame oil. *Journal of Polymers and the Environment, 0123456789*. 10.1007/s10924-021-02119-0.

Hernández-García, E., Vargas, M., & Chiralt, A. (2021). Thermoprocessed starch-polyester bilayer films as affected by the addition of gellan or xanthan gum. *Food Hydrocolloids, 113*(December 2020), Article 106509. 10.1016/j.foodhyd.2020.106509.

Huang, C., & Thomas, N. L. (2018). Fabricating porous poly(lactic acid) fibres via electrospinning. *European Polymer Journal, 99*(December 2017), 464–476. 10.1016/j.eurpolymj.2017.12.025.

Hutchings, J. B. (1999). Instrumental specification. In *Food colour and appearance* (pp. 199–237). Springer US. 10.1007/978-1-4615-2373-4_7.

Jamshidian, M., Tehrany, E. A., Imran, M., Jacquot, M., & Desobry, S. (2010). Poly-lactic acid: Production, applications, nanocomposites, and release studies. *Comprehensive Reviews in Food Science and Food Safety, 9*(5), 552–571. 10.1111/j.1541-4337.2010.00126.x.

La Fuente Arias, C. I., Kubo, M. T. K., Tadini, C. C., & Augusto, P. E. D. (2021). Bio-based multilayer films: A review of the principal methods of production and challenges. *Critical Reviews in Food Science and Nutrition, 0*(0), 1–17. 10.1080/10408398.2021.1973955.

Liu, L., Chen, S., Zhang, X., Xue, Z., Cui, S., Hua, X., et al., (2020). Mechanical penetration of β-lactam–resistant Gram-negative bacteria by programmable nanowires. *Science Advances, 6*(27), 1–13. 10.1126/sciadv.abb9593.

Liu, W., Xie, J., Li, L., Xue, B., Li, X., Gan, J., et al., (2021). Properties of phenolic acid-chitosan composite films and preservative effect on Penaeus vannamei. *Journal of Molecular Structure, 1239*. 10.1016/j.molstruc.2021.130531.

Mahy, M., Van Eycken, L., & Oosterlinck, A. (1994). Evaluation of uniform color spaces developed after the adoption of CIELAB and CIELUV. In *Color research & application: 19* (pp. 105–121). 10.1111/j.1520-6378.1994.tb00070.x.

Mangaraj, S., Yadav, A., Bal, L. M., Dash, S. K., & Mahanti, N. K. (2018). Application of biodegradable polymers in food packaging industry: A comprehensive review. *Journal of Packaging Technology and Research, 3*(1), 77–96 *2018 3:1*. 10.1007/S41783-018-0049-Y.

Miyague, L., Macedo, R. E. F., Meca, G., Holley, R. A., & Luciano, F. B. (2015). Combination of phenolic acids and essential oils against Listeria monocytogenes. *LWT - Food Science and Technology, 64*(1), 333–336. 10.1016/j.lwt.2015.05.055.

Muller, J., González-Martínez, C., & Chiralt, A. (2017). Poly(lactic) acid (PLA) and starch bilayer films, containing cinnamaldehyde, obtained by compression moulding. *European Polymer Journal, 95*(June), 56–70. 10.1016/j.eurpolymj.2017.07.019.

Noubigh, A., & Akremi, A. (2019). Solution thermodynamics of transCinnamic acid in (methanol + water) and (ethanol + water) mixtures at different temperatures. *Journal of Molecular Liquids, 274*, 752–758. 10.1016/j.molliq.2018.09.131.

Ordoñez, R., Atarés, L., & Chiralt, A. (2021). Physicochemical and antimicrobial properties of cassava starch films with ferulic or cinnamic acid. *LWT, 144*(February), Article 111242. 10.1016/j.lwt.2021.111242.

Ordoñez, R., Atarés, L., & Chiralt, A. (2022a). Properties of PLA films with cinnamic acid: Effect of the processing method. *Food and Bioproducts Processing, 3*, 25–33. 10.1016/j.fbp.2022.02.002.

Ordoñez, R., Atarés, L., & Chiralt, A. (2022b). Effect of ferulic and cinnamic acids on the functional and antimicrobial properties in thermo-processed PLA films. *Food Packaging and Shelf Life, 33*, Article 100882. 10.1016/j.fpsl.2022.100882.

Ordoñez, R., Atarés, L., & Chiralt, A. (2022c). Antilisterial action of PLA films with ferulic acid as affected by the method of incorporation. *Food Bioscience, 49*, Article 101865. 10.1016/j.fbio.2022.101865.

Porta, R., Sabbah, M., & Di Pierro, P. (2020). Biopolymers as food packaging materials. *International Journal of Molecular Sciences, 21*(14), 4942. 10.3390/ijms21144942.

Quiles-Carrillo, L., Montanes, N., Lagaron, J. M., Balart, R., & Torres-Giner, S. (2019). Bioactive multilayer polylactide films with controlled release capacity of gallic acid accomplished by incorporating electrospun nanostructured coatings and interlayers. *Applied Sciences (Switzerland), 9*(3). 10.3390/app9030533.

Rashmi, H. B., & Negi, P. S. (2020). Phenolic acids from vegetables: A review on processing stability and health benefits. *Food Research International, 136*, Article 109298. 10.1016/j.foodres.2020.109298.

Rocca-Smith, J. R., Chau, N., Champion, D., Brachais, C. H., Marcuzzo, E., Sensidoni, A., et al., (2017). Effect of the state of water and relative humidity on ageing of PLA films. *Food Chemistry, 236*, 109–119. 10.1016/j.foodchem.2017.02.113.

Shakeel, F., Salem-Bekhit, M. M., Haq, N., & Siddiqui, N. A. (2017). Solubility and thermodynamics of ferulic acid in different neat solvents: Measurement, correlation and molecular interactions. *Journal of Molecular Liquids, 236*, 144–150. 10.1016/j.molliq.2017.04.014.

Tampau, A., González-Martínez, C., & Chiralt, A. (2018). Release kinetics and antimicrobial properties of carvacrol encapsulated in electrospun poly-(ε-caprolactone) nanofibres. Application in starch multilayer films. *Food Hydrocolloids, 79*, 158–169. 10.1016/j.foodhyd.2017.12.021.

Tampau, A., González-Martínez, C., & Chiralt, A. (2020). Polylactic acid–based materials encapsulating carvacrol obtained by solvent casting and electrospinning. *Journal of Food Science, 85*(4), 1177–1185. 10.1111/1750-3841.15094.

Urbaniak-Domagala, W. (2013). Electrical properties of polylactides. *Journal of Electrostatics, 71*(3), 456–461. 10.1016/j.elstat.2013.01.008.

Yildirim, S., Röcker, B., Pettersen, M. K., Nilsen-Nygaard, J., Ayhan, Z., Rutkaite, R., et al., (2018). Active packaging applications for food. *Comprehensive Reviews in Food Science and Food Safety, 17*(1), 165–199. 10.1111/1541-4337.12322.

Yilmaz, M. T., Hassanein, W. S., Alkabaa, A. S., & Ceylan, Z. (2022). Electrospun eugenol-loaded gelatin nanofibers as bioactive packaging materials to preserve quality characteristics of beef. *Food Packaging and Shelf Life, 34*, Article 100968. 10.1016/j.fpsl.2022.100968.

Zhong, Y., Godwin, P., Jin, Y., & Xiao, H. (2020). Biodegradable polymers and green-based antimicrobial packaging materials: A mini-review. *Advanced Industrial and Engineering Polymer Research, 3*(1), 27–35. 10.1016/j.aiepr.2019.11.002.